PID-controlled Particle Swarm Optimization

ZHIHUA CUI[1]*, XINGJUAN CAI[1], JIANCHAO ZENG[1], YUFENG YIN[2]

[1] *Complex System and Computational Intelligence Laboratory, Taiyuan University of Science and Technology, No.66 Waliu Road, Wanbailin District, Taiyuan,Shanxi, China, 030024.*

[2] *School of Mechanical and Electronic Engineering, Taiyuan University of Science and Technology, No.66 Waliu Road, Wanbailin District, Taiyuan,Shanxi, China, 030024.*

Premature convergence is a major challenge for particle swarm optimization algorithm (PSO) when dealing with multi-modal problems. The reason is partly due to the insufficient exploration capability because of the fast convergent speed especially in the final stage. In this paper, the PSO is regarded as a two-inputs one-output feedback system, and two PID controllers are incorporated into the methodology of PSO to improve the population diversity. Different from the integral controller, PID controller has three independent parameters and adjusts them dynamically. Theoretical results with support set theory and stability analysis both demonstrate that PID controller provides more chances to escaping from a local optimum. To validate the efficiency of this new variant, four other famous variants are used to compare including the comprehensive leaning PSO, modified time-varying accelerator coefficients PSO, integral-controlled PSO and the standard version, the test suit consists five unconstrained numerical benchmarks with dimensionality 30 and 100, respectively. Simulation results show PID-controlled PSO is suitable for high-dimensional multi-modal problems due to the large exploration capability in the final stage.

Key words: particle swarm optimization, PID controller, support set theory, stability analysis.

* email: cuizhihua@gmail.com

1 INTRODUCTION

Particle swarm optimization (PSO) [1][2] is a novel stochastic optimization methodology by simulating the animal social behaviors e.g. flocking of birds and schooling of fish. Because of the fast convergent speed and easy implementation, it has been widely applied to many areas, e.g. constrained optimization [3], forecasting problem [4], flow shop scheduling [5] and polygonal approximation of digital curves [6].

In PSO algorithm, each particle represents a potential solution and flies in the search space to seek the food (global optimum). The population is evolved by competition and cooperation among particles.

For each particle, there are two characters: position and velocity. Suppose $\overrightarrow{x}_j(t) = (x_{j1}(t), x_{j2}(t), ..., x_{jn}(t)$ (where n denotes the dimension) is the position vector of particle j in t generation, then it is updated by

$$x_{jk}(t+1) = x_{jk}(t) + v_{jk}(t+1) \tag{1}$$

where $\overrightarrow{v}_j(t) = (v_{j1}(t), v_{j2}(t), ..., v_{jn}(t)$ denotes the velocity information of $j's$ particle at time t, it is evolved according to

$$v_{jk}(t+1) = wv_{jk}(t) + c_1r_1(p_{jk}(t) - x_{jk}(t)) + c_2r_2(p_{gk}(t) - x_{jk}(t)) \tag{2}$$

where $p_{jk}(t)$ means the k^{th} dimensional value of the best position vector which particle j has been found, as well as $p_{gk}(t)$ denotes the corresponding coordinate of the best position found by the entire swarm. Inertia weight w, cognitive learning factor c_1 and social learning factor c_2 are three parameters controlling the size of velocity vector. r_1 and r_2 are two random numbers generated with normal distributions.

To keep the stability of the PSO, a predefined constant v_{max} is used to limit the size of velocity such as:

$$|v_{jk}(t)| \leq v_{max} \tag{3}$$

Similarly with evolutionary computation families, the premature convergence is also a major problem of PSO. Due to the fast convergent speed, PSO may get easily trapped in a local optimum when solving multi-modal problems. To overcome this shortcoming, many strategies have been proposed. By introducing a repulsive motion, Riget [7] designed an attractive and repulsive particle swarm optimization aiming to increase the population diversity. Similarly, He [8] improved the diversity with an additional individual escaping behavior by simulating the original cradle escaping phenomena. Furthermore, Cui [9] incorporated the fitness uniform selection strategy (FUSS) and

"random walk strategy" (RWS) into the PSO methodology, simulation results show it achieves well performance in high-dimensional problems. In the standard version of PSO (SPSO), each particle is attracted by the best locations found by its neighbors and iteself, but Mendes [10] found that the weighted combination of all neighbors may produce a better performance. There are still some other work about this problem, e.g. the alternation of the neighborhood topology[11], the introduction of subpopulation and giving the particles a physical extension[12], etc. Due to the limited space, please refer to the corresponding references.

In 2005, Zeng [13][14] found that the structure of SPSO is equivalent to a two-inputs one-output feedback system, and two integral controllers are incorporated into this methodology to enhance the exploration capability. However, due to the characters of integral controller, it provides a large exploration in the first period, whereas only a weak exploration in the final stage. If SPSO does not locate the region covering the global optimum, it still easily gets trapped into a local optimum. Therefore, in this paper, a new type of controller, PID controller, is used to replace the integral controller due to its complex behavior. For a PID controller, its behavior is dominated by three independent coefficients: K_p, T_I and T_D. This means the exploration capability can be obtained by adjusting these three parameters dynamically.

The rest of this paper was organized as follows. In section 2, we provide a brief introduction to the integral-controlled PSO (ICPSO) [13][14]. It was used as the basis for our novel development, whereas as a comparative measure of performance of the novel method proposed in this paper. In section 3, we introduce the extension to ICPSO proposed in this paper. Experimental settings for the benchmarks and simulation strategies are explained in Section 4, and the results in comparison with four previous developments are also presented in this section. Finally, conclusion and future research are discussed.

2 SOME PREVIOUS WORK

In this paper, only unconstrained optimization problems are considered. Generally, an unconstrained problem can be formulated as a following n-dimensional minimization problem:

$$\min f(\overrightarrow{x}), \quad \overrightarrow{x} = (x_1, x_2, ..., x_n) \in D \subseteq R^n \tag{4}$$

where n is the number of the parameters to be optimized, and D is the search space.

In this section, we give a brief introduction for the method proposed by Zeng and Cui [13][14] which serves as both a basis for and performance gauge of the novel strategies introduced in this paper.

2.1 Control Analysis of SPSO

Substituting Eq. (2) into Eq. (1), and combining the same items, we have

$$x_{jk}(t+1) = (w+1)x_{jk}(t) - wx_{jk}(t-1) + \varphi_1(p_{jk}(t) - x_{jk}(t)) + \varphi_2(p_{gk}(t) - x_{jk}(t)) \quad (5)$$

where $\varphi_1 = c_1 r_1$, $\varphi_2 = c_2 r_2$, and $\varphi = \varphi_1 + \varphi_2$.

For analysis convenience, let φ_1 and φ_2 are two constants, then variable φ is also a constant. Suppose the values of $p_{jk}(t)$ and $p_{gk}(t)$ are generation-independents, then they are denoted as p_{jk} and p_{gk}, applying z-translation into p_{jk} and p_{gk} and resulting

$$P_{jk}(z) = \frac{z}{z-1}p_{jk} \quad P_{gk}(z) = \frac{z}{z-1}p_{gk} \quad (6)$$

With the same z-translation, Eq. (5) is changed to

$$X_{jk}(z) = \frac{z}{z^2 - (w+1)z + w}[\varphi_1(P_{jk}(z) - X_{jk}(z)) + \varphi_2(P_{gk}(z) - X_{jk}(z))] \quad (7)$$

From the control viewpoint, Eq. (7) is a two-inputs one-output feedback system showed in Fig.1.

Fig.1 shows that the sum of cognitive part and social part $\varphi_1(p_{jk}(t) - x_{jk}(t)) + \varphi_2(p_{gk}(t) - x_{jk}(t))$ is the parallel connection of two integral controllers. Since the cognitive part and social part influence the performance significantly, one intuitive and simple method is the introduction of other type controllers may provide an interesting work(showed in Fig.2).

2.2 Integral-controlled PSO

Integral-controlled particle swarm optimization (ICPSO) is a special case of Fig.2 with two controllers are both set to integral controller. Because the z-translation of integral controller is $\frac{z}{z-1}$, substituting it into Fig.2 and resulting

$$X_{jk}(z) = \frac{z^2}{z^3 - (w+2)z^2 + (2w+1)z - w}[\varphi_1(P_{jk}(z) - X_{jk}(z)) + \varphi_2(P_{gk}(z) - X_{jk}(z))] \quad (8)$$

Applying inverse z-translation, the following update equation is obtained:

$$x_{jk}(t+1) = (w+2)x_{jk}(t) - (2w-1)x_{jk}(t-1) + wx_{jk}(t-2) + \varphi_1(p_{jk}(t) - x_{jk}(t)) + \varphi_2(p_{gk}(t) - x_{jk}(t)) \quad (9)$$

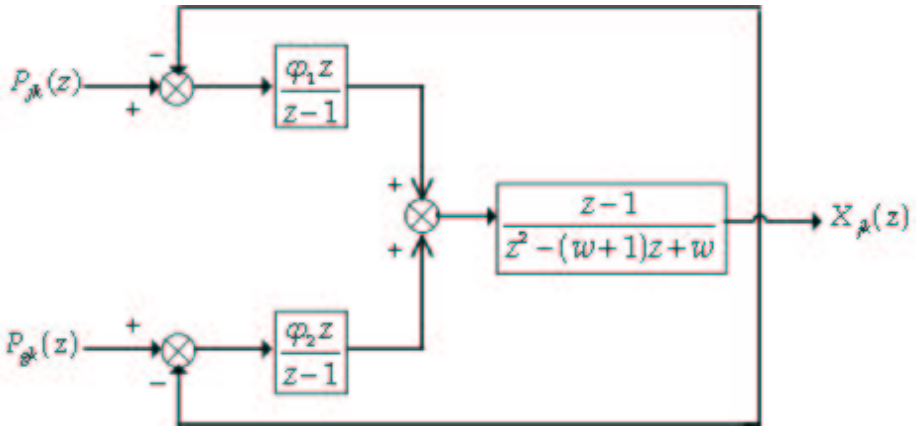

FIGURE 1
System Diagram of Standard PSO.

Defining:

$$v_{jk}(t+1) = x_{jk}(t+1) - x_{jk}(t) \tag{10}$$

$$\begin{aligned} a_{jk}(t+1) &= v_{jk}(t+1) - v_{jk}(t) \\ &= x_{jk}(t+1) - 2x_{jk}(t) + x_{jk}(t-1) \end{aligned} \tag{11}$$

Then, the final update equations of integral-controlled particle swarm optimization are:

$$a_{jk}(t+1) = wa_{jk}(t) + \varphi_1(p_{jk}(t) - x_{jk}(t)) + \varphi_2(p_{gk}(t) - x_{jk}(t)) \tag{12}$$

$$v_{jk}(t+1) = v_{jk}(t) + a_{jk}(t+1) \tag{13}$$

$$x_{jk}(t+1) = x_{jk}(t) + v_{jk}(t+1) \tag{14}$$

The difference between integral-controlled PSO and the standard PSO is only the introduction of accelerator information. Therefore, the evolutionary behavior of ICPSO is more complex than that of SPSO because ICPSO is a three-order system, nor a two-order system.

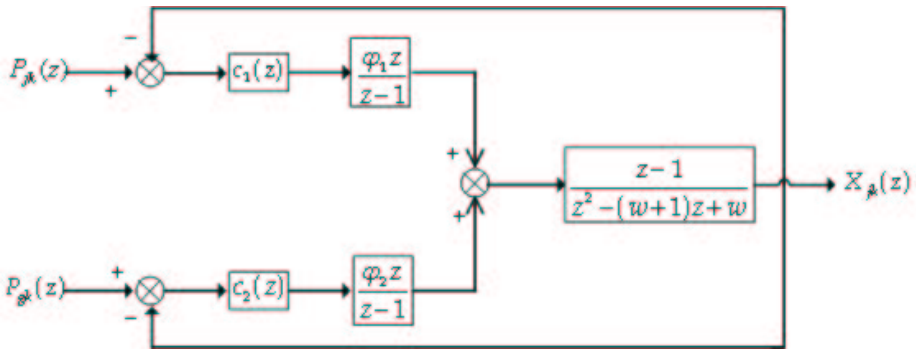

FIGURE 2
System Diagram of the Integral- controlled PSO.

The integral term considers the history of the error, or how long and how far the measured process variable has been from the set point over time. Here, the error denotes the distance between the current position and the historical best position found the particle's neighbors. It is obviously that if the error tends to zero, the search of ICPSO will be stopped, this may lead to premature convergence if the global optimum is still not find. This character of integral controll illustrates why ICPSO still gets trapped to a local optimum. To overcome this shortcoming, PID controller is introduced to improve the performance of ICPSO.

3 PID-CONTROLLED PSO

3.1 Update Equations

In this section, a new controller, PID controller, is introduced to construct a new variant – PID-controlled particle swarm optimization (PID-PSO).

Different from integral controller, the z-translation of PID controller is

$$K_p(1 + \frac{z}{T_I(z-1)} + T_D\frac{z-1}{z}) \tag{15}$$

where proportional gain K_p, integral gain T_I and derivative gain T_D are three new parameters.

Applying $c_1(z) = c_2(z) = K_p(1 + \frac{z}{T_I(z-1)} + T_D\frac{z-1}{z})$ into the methodology of PSO, resulting

$$X_{jk}(z) = \frac{z}{z^2-(w+1)z+w} \cdot K_p \cdot [1 + \frac{z}{T_I(z-1)} + T_D\frac{z-1}{z}] \quad (16)$$
$$= \frac{K_p}{T_I} \cdot \frac{(T_I+1+T_DT_I)z^2 - (T_I+2T_DT_I)z + T_DT_I}{[z^2-(w+1)z+w]\cdot(z-1)} \cdot u(z)$$

where $u(z) = \varphi_1(P_{jk}(z) - X_{jk}(z)) + \varphi_2(P_{gk}(z) - X_{jk}(z))$.

Suppose $\alpha = T_I + T_DT_I + 1$, $\beta = -(T_I + 2T_DT_I)$, $\gamma = T_DT_I$, $\varphi_1^{'} = \frac{K_p}{T_I}\varphi_1$, and $\varphi_2^{'} = \frac{K_p}{T_I}\varphi_2$, then Eq. (16) is rewritten as

$$X_{jk}(z) = \frac{\alpha z^2 + \beta z}{z^3-(w+2)z^2+(2w+1)z-w}[\varphi_1^{'}(P_{jk}(z) - X_{jk}(z)) \quad (17)$$
$$+\varphi_2^{'}(P_{gk}(z) - X_{jk}(z))]$$

Applying inverse z-translation, then the update equation is

$$x_{jk}(t+1) - (w+2)x_{jk}(t) + (2w+1)x_{jk}(t-1) - wx_{jk}(t-2) \quad (18)$$
$$= \alpha\varphi_1^{'}[p_{jk}(t) - x_{jk}(t)] + \alpha\varphi_2^{'}[p_{gk}(t) - x_{jk}(t)]$$
$$+\beta\varphi_1^{'}[p_{jk}(t-1) - x_{jk}(t-1)] + \beta\varphi_2^{'}[p_{gk}(t-1) - x_{jk}(t-1)]$$
$$+\gamma\varphi_1^{'}[p_{jk}(t-2) - x_{jk}(t-2)] + \gamma\varphi_2^{'}[p_{gk}(t-2) - x_{jk}(t-2)]$$

Similar with ICPSO, defining:

$$v_{jk}(t+1) = x_{jk}(t+1) - x_{jk}(t) \quad (19)$$

and

$$a_{jk}(t+1) = v_{jk}(t+1) - v_{jk}(t) = x_{jk}(t+1) - 2x_{jk}(t) + x_{jk}(t-1) \quad (20)$$

Then, the final update equations of PID-PSO are obtained as follows:

$$a_{jk}(t+1) = wa_{jk}(t) + \alpha\varphi_1^{'}(p_{jk}(t) - x_{jk}(t)) + \alpha\varphi_2^{'}(p_{gk}(t) - x_{jk}(t)) \quad (21)$$
$$+\beta\varphi_1^{'}[p_{jk}(t-1) - x_{jk}(t-1)] + \beta\varphi_2^{'}[p_{gk}(t-1) - x_{jk}(t-1)]$$
$$+\gamma\varphi_1^{'}[p_{jk}(t-2) - x_{jk}(t-2)] + \gamma\varphi_2^{'}[p_{gk}(t-2) - x_{jk}(t-2)]$$

$$v_{jk}(t+1) = v_{jk}(t) + a_{jk}(t+1) \quad (22)$$

$$x_{jk}(t+1) = x_{jk}(t) + v_{jk}(t+1) \quad (23)$$

Eq. (21)-(23) illustrate the behavior of PID-PSO is also a three-order system, however, difference from ICPSO, there are three additional parameters used to control the trajectory of each particle.

3.2 Support Set Theory Analysis

In convergence theory of PSO, the support set $M_{j,t}$[15] is an important statistic reflecting how large the population diversity is, if the search space is covered by the union of the sample space of all particles, in other words, $D \subseteq \bigcup_j M_{j,t}$, PSO is convergent to the global optimum with probability one. Generally, the larger support set $M_{j,t}$ is, the better convergence performance maintains, and vice versa. For SPSO, the support set $M_{j,t}$ is

$$M_{j,t} = (w+1)\overrightarrow{x}_j(t-1) - w\overrightarrow{x}_j(t-2) + \varphi_1(\overrightarrow{p}_j(t-1) - \overrightarrow{x}_{j-1}) + \varphi_2(\overrightarrow{p}_g(t-1) - \overrightarrow{x}_{j-1}) \quad (24)$$

Considering the range of $\varphi_1(\in [0, c_1])$ and $\varphi_2(\in [0, c_2])$, $M_{j,t}$ is a hyper-rectangle by φ_1 and φ_2, with one corner specified by $\varphi_1 = \varphi_2 = 0$, and the other by $\varphi_1 = c_1$ and $\varphi_2 = c_2$.

If $\varphi_1 = \varphi_2 = 0$, the support set is

$$M^0_{j,t} = (w+1)\overrightarrow{x}_j(t-1) - w\overrightarrow{x}_j(t-2) \quad (25)$$

and when $\varphi_1 = c_1$ and $\varphi_2 = c_2$ are satisfied, the support set is changed to

$$M^c_{j,t} = (w+1)\overrightarrow{x}_j(t-1) - w\overrightarrow{x}_j(t-2) + c_1(\overrightarrow{p}_j(t-1) - \overrightarrow{x}_{j-1}) + c_2(\overrightarrow{p}_g(t-1) - \overrightarrow{x}_{j-1}) \quad (26)$$

To provide a measurement for support set of each particle, the diagonal line is used. For the standard version of PSO, the diagonal line is

$$M^c_{j,t} - M^0_{j,t} = c_1(\overrightarrow{p}_j(t-1) - \overrightarrow{x}_{j-1}) + c_2(\overrightarrow{p}_g(t-1) - \overrightarrow{x}_{j-1}) \quad (27)$$

In Euclid space R^n, all norms are equivalents. In this paper, only the $\infty-$norm is considered. The $\infty-$norm of Eq. (27) is

$$Length_{PSO} = \max_{1\le k\le n}\{|c_1(p_{jk}(t-1) - x_{jk}(t-1)) + c_2(p_{gk}(t-1) - x_{jk}(t-1))|\} \quad (28)$$

For convenience, dimension s is chosen and the Eq.(28) is rewritten by

$$\begin{aligned} Length_{PSO} &= |c_1(p_{js}(t-1) - x_{js}(t-1)) + c_2(p_{gs}(t-1) - x_{js}(t-1))| \quad (29)\\ &= \max_{1\le k\le n}\{|c_1(p_{jk}(t-1) - x_{jk}(t-1)) + c_2(p_{gk}(t-1) - x_{jk}(t-1))|\} \end{aligned}$$

Eq.(29) provides a roughly measure for the support set of SPSO, the following part will discuss the support set of PID-PSO, and provide a detailed comparison.

For PID-PSO algorithm, the support set $M_{j,t}^{'}$ of particle j is

$$\begin{aligned} M_{j,t}^{'} &= (w+2)\overrightarrow{x}_j(t-1) - (2w+1)\overrightarrow{x}_j(t-2) + w\overrightarrow{x}_j(t-3) \\ &+\alpha\varphi_1^{'}[\overrightarrow{p}_j(t-1) - \overrightarrow{x}_j(t-1)] + \alpha\varphi_2^{'}[\overrightarrow{p}_g(t-1) - \overrightarrow{x}_j(t-1)] \\ &+\beta\varphi_1^{'}[\overrightarrow{p}_j(t-2) - \overrightarrow{x}_j(t-2)] + \beta\varphi_2^{'}[\overrightarrow{p}_g(t-2) - \overrightarrow{x}_j(t-2)] \\ &+\gamma\varphi_1^{'}[\overrightarrow{p}_j(t-3) - \overrightarrow{x}_j(t-3)] + \gamma\varphi_2^{'}[\overrightarrow{p}_g(t-3) - \overrightarrow{x}_j(t-3)] \end{aligned} \quad (30)$$

where $0 \leq \varphi_1^{'} \leq \frac{K_p}{T_I}c_1$, $0 \leq \varphi_2^{'} \leq \frac{K_p}{T_I}c_2$. Support set $M_{j,t}^{'}$ is a hyper-rectangle by $\varphi_1^{'}$ and $\varphi_2^{'}$, with one corner specified by $\varphi_1^{'} = \varphi_2^{'} = 0$, and the other by $\varphi_1^{'} = \frac{K_p}{T_I}c_1$ and $\varphi_2^{'} = \frac{K_p}{T_I}c_2$.

If $\varphi_1^{'} = \varphi_2^{'} = 0$ is true, the support set is

$$M_{j,t}^{0'} = (w+2)\overrightarrow{x}_j(t-1) - (2w+1)\overrightarrow{x}_j(t-2) + w\overrightarrow{x}_j(t-3) \quad (31)$$

and when $\varphi_1^{'} = \frac{K_p}{T_I}c_1$ and $\varphi_2^{'} = \frac{K_p}{T_I}c_2$ are satisfied, the support set is changed to

$$\begin{aligned} M_{j,t}^{c'} &= (w+2)\overrightarrow{x}_j(t-1) - (2w+1)\overrightarrow{x}_j(t-2) + w\overrightarrow{x}_j(t-3) \\ &+\alpha\frac{K_p}{T_I}c_1[\overrightarrow{p}_j(t-1) - \overrightarrow{x}_j(t-1)] + \alpha\frac{K_p}{T_I}c_2[\overrightarrow{p}_g(t-1) - \overrightarrow{x}_j(t-1)] \\ &+\beta\frac{K_p}{T_I}c_1[\overrightarrow{p}_j(t-2) - \overrightarrow{x}_j(t-2)] + \beta\frac{K_p}{T_I}c_2[\overrightarrow{p}_g(t-2) - \overrightarrow{x}_j(t-2)] \\ &+\gamma\frac{K_p}{T_I}c_1[\overrightarrow{p}_j(t-3) - \overrightarrow{x}_j(t-3)] + \gamma\frac{K_p}{T_I}c_2[\overrightarrow{p}_g(t-3) - \overrightarrow{x}_j(t-3)] \end{aligned} \quad (32)$$

The diagonal line of support set $M_{j,t}^{'}$ is

$$\begin{aligned} M_{j,t}^{c'} - M_{j,t}^{0'} &= \alpha\frac{K_p}{T_I}c_1[\overrightarrow{p}_j(t-1) - \overrightarrow{x}_j(t-1)] + \alpha\frac{K_p}{T_I}c_2[\overrightarrow{p}_g(t-1) - \overrightarrow{x}_j(t-1)] \\ &+\beta\frac{K_p}{T_I}c_1[\overrightarrow{p}_j(t-2) - \overrightarrow{x}_j(t-2)] + \beta\frac{K_p}{T_I}c_2[\overrightarrow{p}_g(t-2) - \overrightarrow{x}_j(t-2)] \\ &+\gamma\frac{K_p}{T_I}c_1[\overrightarrow{p}_j(t-3) - \overrightarrow{x}_j(t-3)] + \gamma\frac{K_p}{T_I}c_2[\overrightarrow{p}_g(t-3) - \overrightarrow{x}_j(t-3)] \end{aligned} \quad (33)$$

Calculating the $\infty-$norm and resulting

$$\begin{aligned} & Length_{PID-PSO} \\ &= \max_{1\leq k\leq n}\{|\alpha\frac{K_p}{T_I}c_1[p_{jk}(t-1) - x_{jk}(t-1)] + \alpha\frac{K_p}{T_I}c_2[p_{gk}(t-1) - x_{jk}(t-1)] \\ &+\beta\frac{K_p}{T_I}c_1[p_{jk}(t-2) - x_{jk}(t-2)] + \beta\frac{K_p}{T_I}c_2[p_{gk}(t-2) - x_{jk}(t-2)] \\ &+\gamma\frac{K_p}{T_I}c_1[p_{jk}(t-3) - x_{jk}(t-3)] + \gamma\frac{K_p}{T_I}c_2[p_{gk}(t-3) - x_{jk}(t-3)]|\} \end{aligned} \quad (34)$$

Generally, the parameters K_p, T_I and T_D are all positive, it means α and γ are non-negative, β is non-positive. Hence, Eq.(34) is rewritten with the following manner:

$$Length_{PID-PSO} \quad (35)$$
$$= \frac{K_p}{T_I} \cdot \max_{1\le k\le n} \{|\alpha c_1[p_{jk}(t-1) - x_{jk}(t-1)] + \alpha c_2[p_{gk}(t-1) - x_{jk}(t-1)]$$
$$+\beta c_1[p_{jk}(t-2) - x_{jk}(t-2)] + \beta c_2[p_{gk}(t-2) - x_{jk}(t-2)]$$
$$+\gamma c_1[p_{jk}(t-3) - x_{jk}(t-3)] + \gamma c_2[p_{gk}(t-3) - x_{jk}(t-3)]|\}$$

The lower bounds of $Length_{PID-PSO}$ is estimated by

$$Length_{PID-PSO} \quad (36)$$
$$\ge \frac{K_p}{T_I} \cdot \{|\alpha c_1[p_{js}(t-1) - x_{js}(t-1)] + \alpha c_2[p_{gs}(t-1) - x_{js}(t-1)]$$
$$+\beta c_1[p_{js}(t-2) - x_{js}(t-2)] + \beta c_2[p_{gs}(t-2) - x_{js}(t-2)]$$
$$+\gamma c_1[p_{js}(t-3) - x_{js}(t-3)] + \gamma c_2[p_{gs}(t-3) - x_{js}(t-3)]|\}$$

Suppose

$$u_1 = c_1[p_{js}(t-1) - x_{js}(t-1)] + c_2[p_{gs}(t-1) - x_{js}(t-1)] \quad (37)$$

$$u_2 = c_1[p_{js}(t-2) - x_{js}(t-2)] + c_2[p_{gs}(t-2) - x_{js}(t-2)] \quad (38)$$

and

$$u_3 = c_1[p_{js}(t-3) - x_{js}(t-3)] + c_2[p_{gs}(t-3) - x_{js}(t-3)] \quad (39)$$

Then, Eq.(36) is written by u_1, u_2 and u_3:

$$Length_{PID-PSO} \ge \frac{K_p}{T_I} \cdot |\alpha u_1 + \beta u_2 + \gamma u_3| \quad (40)$$

Furthermore, the upper bound of $Length_{PID-PSO}$ is

$$Length_{PID-PSO} \quad (41)$$
$$\le \frac{K_p}{T_I} \cdot \max_{1\le k\le n} \{|\alpha c_1[p_{jk}(t-1) - x_{jk}(t-1)] + \alpha c_2[p_{gk}(t-1) - x_{jk}(t-1)]|$$
$$+|\beta c_1[p_{jk}(t-2) - x_{jk}(t-2)] + \beta c_2[p_{gk}(t-2) - x_{jk}(t-2)]|$$
$$+|\gamma c_1[p_{jk}(t-3) - x_{jk}(t-3)] + \gamma c_2[p_{gk}(t-3) - x_{jk}(t-3)]|\}$$
$$\le \frac{K_p}{T_I} \cdot \max_{1\le k\le n} \{|\alpha c_1[p_{jk}(t-1) - x_{jk}(t-1)] + \alpha c_2[p_{gk}(t-1) - x_{jk}(t-1)]|\}$$

$$
\begin{aligned}
&+ \max_{1\le k\le n}\{|\beta c_1[p_{jk}(t-2) - x_{jk}(t-2)] + \beta c_2[p_{gk}(t-2) - x_{jk}(t-2)]|\} \\
&+ \max_{1\le k\le n}\{|\gamma c_1[p_{jk}(t-3) - x_{jk}(t-3)] + \gamma c_2[p_{gk}(t-3) - x_{jk}(t-3)]|\} \\
&= \frac{K_p}{T_I}\cdot\{|\alpha u_1| + |\beta u_2^{'}| + |\gamma u_3^{'}|\} \\
&= \frac{K_p}{T_I}\cdot\{\alpha|u_1| - \beta|u_2^{'}| + \gamma|u_3^{'}|\}
\end{aligned}
$$

where

$$
u_2^{'} = \max_{1\le k\le n}\{\alpha c_1[p_{jk}(t-2) - x_{jk}(t-2)] + |\alpha c_2[p_{gk}(t-2) - x_{jk}(t-2)]\} \quad (42)
$$

$$
u_3^{'} = \max_{1\le k\le n}\{\alpha c_1[p_{jk}(t-3) - x_{jk}(t-3)] + |\alpha c_2[p_{gk}(t-3) - x_{jk}(t-3)]\} \quad (43)
$$

Obviously, the value $Length_{PSO}$ (Eq.29) is

$$
Length_{PSO} = |u_1| \quad (44)
$$

Because the introduction of PID controller tends to increase the exploration capability especially in the final stage, therefore, we will discuss whether there exist such parameter combinations for PID-PSO.

After simple calculation, there are no parameters values for α, β and γ such that the $\alpha u_1 \times (\beta u_2 + \gamma u_3) > 0$ holds if one of the following conditions is true:

$$
\begin{cases}
u_1 > 0 \\
u_2 \ge 0 \\
u_3 \le 2u_2
\end{cases} \quad (45)
$$

$$
\begin{cases}
u_1 < 0 \\
u_2 \le 0 \\
u_3 \ge 2u_2
\end{cases} \quad (46)
$$

In other words, if the condition (45) and (46) are both not satisfied, then there exists α, β and γ such that

$$
\alpha u_1 \times (\beta u_2 + \gamma u_3) > 0 \quad (47)
$$

For convinence, let $\alpha u_1 > 0$, then we can choice the parameter β and γ, making $\beta u_2 + \gamma u_3 > 0$ is true. In this case, the lower bound of Eq.(40) is changed to

$$
Length_{PID-PSO} \quad (48)
$$

$$
\begin{aligned}
&\geq \frac{K_p}{T_I} \cdot |\alpha u_1 + \beta u_2 + \gamma u_3| \\
&\geq \frac{K_p}{T_I} \cdot |\alpha u_1| + |\beta u_2 + \gamma u_3| \\
&= \frac{K_p}{T_I} \cdot \alpha |u_1| + |\beta u_2 + \gamma u_3|
\end{aligned}
\tag{49}
$$

So,

$$
\begin{aligned}
&Length_{PID-PSO} - Length_{PSO} \\
&\geq (\alpha \frac{K_p}{T_I} - 1) \cdot |u_1| + \frac{K_p}{T_I} \cdot |\beta u_2 + \gamma u_3|
\end{aligned}
\tag{50}
$$

Let

$$
\alpha \frac{K_p}{T_I} - 1 \geq 0 \tag{51}
$$

Then

$$
Length_{PID-PSO} \geq Length_{PSO} \tag{52}
$$

Besides, if one of the conditions (45) and (46) is satisfied, for any parameter α, β and γ, the following inequation is true:

$$
\alpha u_1 \times (\beta u_2 + \gamma u_3) < 0 \tag{53}
$$

From the upper bound of $Length_{PID-PSO}$ (Eq. (41)), we have

$$
\begin{aligned}
&Length_{PSO} - Length_{PID-PSO} \\
&\geq (1 - \frac{K_p}{T_I}\alpha)|u_1| + \frac{K_p}{T_I}[\beta |u_2^{'}| - \gamma |u_3^{'}|]
\end{aligned}
\tag{54}
$$

Eq.(54) implies that $Length_{PSO} - Length_{PID-PSO} \geq 0$ if and only if

$$
(1 - \frac{K_p}{T_I}\alpha)|u_1| + \frac{K_p}{T_I}[\beta |u_2^{'}| - \gamma |u_3^{'}|] > 0 \tag{55}
$$

Rewritten it and resulting

$$
K_p\{|u_1| + |u_2^{'}| + T_D[|u_1| + 2|u_2^{'}| + |u_3^{'}|] + \frac{|u_1|}{T_I}\} \leq |u_1| \tag{56}
$$

Because $u_1 \neq 0$, and

$$
|u_1| + |u_2^{'}| + T_D[|u_1| + 2|u_2^{'}| + |u_3^{'}|] + \frac{|u_1|}{T_I} > 0 \tag{57}
$$

Then,

$$Length_{PSO} \geq Length_{PID-PSO} \tag{58}$$

is true if the parameter K_p follows:

$$K_p \leq \frac{|u_1|}{|u_1| + |u_2'| + T_D[|u_1| + 2|u_2'| + |u_3'|] + \frac{|u_1|}{T_I}} \tag{59}$$

Eqs.(51) and (59) are two conditions used to guide the selection of K_p, T_I and T_D for a larger exploration of PID-PSO when compared with the standard of PSO. If we need a large exploration, the condition (51) should be followed, otherwise, Eq. (59) is used to select the corresponding parameters. In the following part, we will discuss how much probability of conditions (51) and (59) are true?

Suppose $\overrightarrow{p}_j(t) = (p_{j1}(t), p_{j2}(t), ..., p_{jn}(t))$, $\overrightarrow{p}_g(t) = (p_{g1}(t), p_{g2}(t), ..., p_{gn}(t))$ and $\overrightarrow{x}_j(t) = (x_{j1}(t), x_{j2}(t), ..., x_{jn}(t))$ are sampled with uniform distribution in the search space $D = [x_{min}, x_{max}]^n$, according to the definitions of u_1, u_2 and u_3, we have

$$(c_1 + c_2) \cdot (x_{min} - x_{max}) \leq u_1, u_2, u_3 \leq (c_1 + c_2) \cdot (x_{max} - x_{min}) \tag{60}$$

This implies the probability of following four cases are both the same to 25%.

$$u_1 > 0 \quad .and. \quad u_2 \geq 0 \tag{61}$$

$$u_1 < 0 \quad .and. \quad u_2 \leq 0 \tag{62}$$

$$u_1 \leq 0 \quad .and. \quad u_2 > 0 \tag{63}$$

$$u_1 \geq 0 \quad .and. \quad u_2 < 0 \tag{64}$$

For the probability of inequality $u_3 - 2u_2 \geq 0$, we have

$$Pro\{u_3 - 2u_2 \geq 0\} = \int_{(c_1+c_2)\cdot(x_{min}-x_{max})}^{(c_1+c_2)\cdot(x_{max}-x_{min})} du_2 \int_{(c_1+c_2)\cdot(x_{min}-x_{max})}^{2u_2} du_3 = 0.5 \tag{65}$$

Therefore, the conditions of (45) and (46) are true with the following probability:

$$\begin{aligned} Pro &= Pro\{u_1 > 0, u_2 \geq 0\} Pro\{u_3 \leq 2u_2\} + Pro\{u_1 < 0, u_2 \leq 0\} Pro\{u_3 \geq 2u_2\} \\ &= 25\% \cdot 50\% + 25\% \cdot 50\% = 25\% \end{aligned} \tag{66}$$

It means Eq.(51) is true with a probability 75%, and the exloration capability of PID-PSO is smaller than that of the standard PSO with probability 25%. This phenomenon shows that PID-PSO maintains a powerful global search capability, and has more chances to escape from a local optimum.

3.3 Stability Theory Analysis

In this section, the stability theory is used to guide the selection of inertia weight. In PID-PSO, the open-loop z-translation function $G_k(z)$ of $P_{jk}(z)$ is:

$$\begin{aligned} G_k(z) \quad (67)\\ = K_p \cdot [1 + \frac{z}{T_I(z-1)} + T_D \cdot \frac{z-1}{z}] \cdot \frac{\varphi_1 z}{z-1} \cdot \frac{z-1}{z^2-(w+1)z+w} \\ = \frac{K_p}{T_I} \cdot \varphi_1 \cdot \frac{\alpha z^2 + \beta z + \gamma}{(z-1)[z^2-(w+2)z+w]} \\ = \varphi_1^{'} \cdot \frac{\alpha z^2 + \beta z + \gamma}{z^3-(w+2)z^2+(2w+1)z-w} \end{aligned}$$

The characteristic equation of $G_k(z)$ is

$$1 + G_k(z) = 0 \tag{68}$$

It can be rewritten by

$$z^3 - (w+2)z^2 + (2w+1)z - w + \varphi_1^{'} \cdot (\alpha z^2 + \beta z + \gamma) = 0 \tag{69}$$

Applying the translation $z = \frac{y+1}{y-1}$, then Eq.(69) is changed to

$$\begin{aligned} \varphi_1^{'} \cdot y^3 + (2T_I+1)\varphi_1^{'} \cdot y^2 + [4(1-w) + (4T_D T_I - 1)\varphi_1^{'}] \cdot y \quad (70)\\ +[4(1+w) - (1+2T_I+4T_D T_I)\varphi_1^{'}] = 0 \end{aligned}$$

For a general characteristic equation

$$b_0 y^3 + b_1 y^2 + b_2 y + b_3 = 0 \tag{71}$$

According to the Rough stability conditions, this system is stable if and only if the following conditions are met:

$$b_0 > 0, b_1 > 0, b_2 > 0, b_3 > 0, b_1 b_2 - b_0 b_3 > 0 \tag{72}$$

Substituting the conditions (72) into Eq.(70) resulting

$$b_0 > 0 \Rightarrow \varphi_1^{'} = \varphi_1 \frac{K_p}{T_I} > 0 \tag{73}$$

$$b_1 > 0 \Rightarrow (2T_I + 1)\varphi_1^{'} > 0 \tag{74}$$

$$b_2 > 0 \Rightarrow 4(1-w) + (4T_D T_I - 1)\varphi_1^{'} > 0 \tag{75}$$

$$b_3 > 0 \Rightarrow 4(1-w) - (2T_I + 4T_D T_I + 1)\varphi_1^{'} > 0 \tag{76}$$

$$b_1 b_2 - b_0 b_3 > 0 \Rightarrow 8\varphi_1^{'}[T_I - T_I w - w + \varphi_1^{'} T_D T_I (T_I + 1)] > 0 \tag{77}$$

Obviously, Eq.(73) and Eq.(74) are always true. Fron Eqs.(75) and (76), we have

$$\frac{\varphi_1^{'}(2T_I + 4T_D T_I + 1)}{4} - 1 < w < \frac{\varphi_1^{'}(4T_D T_I - 1)}{4} + 1 \tag{78}$$

From Eq.(77), we have

$$w < \frac{T_I}{T_I + 1} + \varphi_1 K_p T_D \tag{79}$$

So,

$$\frac{\varphi_1^{'}(2T_I + 4T_D T_I + 1)}{4} - 1 < w < \min\{\frac{\varphi_1^{'}(4T_D T_I - 1)}{4} + 1, \frac{T_I}{T_I + 1} + \varphi_1 K_p T_D\} \tag{80}$$

With the same analysis, the parameter w is restricted by the following condition also according to the input $P_{gk}(z)$:

$$\frac{\varphi_2^{'}(2T_I + 4T_D T_I + 1)}{4} - 1 < w < \min\{\frac{\varphi_2^{'}(4T_D T_I - 1)}{4} + 1, \frac{T_I}{T_I + 1} + \varphi_2 K_p T_D\} \tag{81}$$

Therefore, if the inertia weight w is satisfied with the conditions (80) and (81), the trajectory of each particle will be convergent onto $\overrightarrow{p}_g$ under the stable conditions of $\beta, \beta, \gamma, K_p, T_I$ and T_D. It means

$$lim_{t\to\infty} \overrightarrow{x}_j(t) = lim_{z\to 1}(z-1)X_j(z) \tag{82}$$

$$lim_{z\to 1}(z-1)\frac{(\alpha z^2 + \beta z + \gamma)(\varphi_1^{'}\overrightarrow{p}_j(z) + \varphi_2^{'}\overrightarrow{p}_g(z))}{z^3 - [w + 2 - \alpha(\varphi_1^{'} + \varphi_2^{'})]z^2 + [2w + 1 + \beta(\varphi_1^{'} + \varphi_2^{'})]z - w + \gamma(\varphi_1^{'} + \varphi_2^{'})}$$

$$lim_{z\to 1}\frac{(\alpha z^2 + \beta z + \gamma)(\varphi_1^{'}\overrightarrow{p}_j z + \varphi_2^{'}\overrightarrow{p}_g z)}{z^3 - [w + 2 - \alpha(\varphi_1^{'} + \varphi_2^{'})]z^2 + [2w + 1 + \beta(\varphi_1^{'} + \varphi_2^{'})]z - w + \gamma(\varphi_1^{'} + \varphi_2^{'})}$$

$$= \frac{(\varphi_1^{'}\overrightarrow{p}_j + \varphi_2^{'}\overrightarrow{p}_g)(\alpha + \beta + \gamma)}{(\varphi_1^{'} + \varphi_2^{'})(\alpha + \beta + \gamma)}$$

$$= \frac{\varphi_1\overrightarrow{p}_j + \varphi_2\overrightarrow{p}_g}{\varphi_1 + \varphi_2}$$

This imples

$$lim_{t\to\infty}\overrightarrow{x}_j(t) = \overrightarrow{p}_j = \overrightarrow{p}_g \tag{83}$$

3.4 Parameter Selection

To escape from a local optimum, PID controllers are introduced to replace the integral controllers. Different from integral controller, the bahavior of each particle is guided by three additional parameters: K_p, T_I and T_D, therefore, PID-PSO maintains a powerful exploration capability by employing different parameters combinations.

K_p is known as the proportional gain, generally, larger values typically mean faster response since the larger the error, the larger the proportional term compensation. An excessively large proportional gain will lead to process instability and oscillation. In PSO methodology, the population diversity plays an important role dominating the success probability escaping from a local optimum. Therefore, the existing errors may provide this chance, so, K_p is setting to

$$K_p(t) = 1.0 - \frac{t}{T} \tag{84}$$

where T is the maximum generation.

Integral gain T_I represents the response speed. Larger values imply steady state errors are eliminated more quickly. The trade-off is larger overshoot: any negative error integrated during transient response must be integrated away by positive error before we reach steady state. With the above mentioned reason, the existing error may provide more chances to escape from a local optimum, so, T_I is setting as follows:

$$T_I(t) = 2.0 - \frac{t}{T} \tag{85}$$

Derivative gain T_D decrease overshoot, but slows down transient response and may lead to instability due to signal noise amplification in the differentiation of the error. To make a large exploration capability, the influence of T_D should be omiited in the final stage. Therefore, in this paper, it is chosen as follows:

$$T_D(t) = 1.0 - \frac{t}{T} \tag{86}$$

The pseudo-code for PID-PSO is illustrated as follows:

Step1. Initializing all parameters, the position vector, velocity vector and accelerator vector of each component of each particle, determining the personal best location and the best location among the entire swarm;

Step2. Updating the accelerator vector, velocity vector and position vector of each particle of the swarm according to equation (21)-(23);

Step3. Determining the personal best location and the best position of the entire swarm;

Step4. If the stop criteria is satisfied, output the obtained best solution; otherwise, goto Step2.

4 SIMULATION RESULTS

To testify the performance of our modification, five famous benchmark functions are chosen to test the performance, and compared with standard PSO (SPSO), modified PSO with time-varying accelerator coefficients (MPSO-TVAC)[16], comprehensive learning PSO (CLPSO)[17] and integral-controlled PSO (ICPSO)[13][14].

In this paper, Rosenbrock, Rastrigin, Ackley and two Penalized Functions are used to test, all of them are multi-modal functions with many local optima except for Rosenbrock[18]. Generally, Rosenbrock is viewed as a unimodal function, however, in recent literatures, several numerical experiments[19] have been made to show Rosenbrock is a multi-modal function with only two local optima when dimensionality between 4 to 30.

Rosenbrock Function:

$$f_1(x) = \sum_{j=1}^{n-1}[100(x_{j+1} - x_j^2)^2 + (x_j - 1)^2]$$

where $|x_j| \leq 30.0$, and

$$f_1(x^*) = f_1(1, 1, ..., 1) = 0.0$$

Rastrigin Function:

$$f_2(x) = \sum_{j=1}^{n}[x_j^2 - 10cos(2\pi x_j) + 10]$$

where $|x_j| \leq 5.12$, and

$$f_2(x^*) = f_2(0, 0, ..., 0) = 0.0$$

Ackley Function:

$$f_3(x) = -20exp(-0.2\sqrt{\frac{1}{n}\sum_{j=1}^{n}x_j^2}) - exp(\frac{1}{n}\sum_{k=1}^{n}\cos 2\pi x_k) + 20 + e$$

where $|x_j| \leq 32.0$, and

$$f_3(x^*) = f_3(0, 0, ..., 0) = 0.0$$

Penalized Function1:

$$f_4(x) = \frac{\pi}{30}\{10\sin^2(\pi y_1) + \sum_{i=1}^{n-1}(y_i - 1)^2[1 + 10\sin^2(\pi y_{i+1})] + (y_n - 1)^2\} + \sum_{i=1}^{n} u(x_i, 10, 100, 4)$$

where $|x_j| \leq 50.0$, and

$$u(x_i, a, k, m) = \begin{cases} k(x_i - a)^m, & \text{if } x_i > a \\ 0, & \text{if } -a \leq x_i \leq a \\ k(-x_i - a)^m, & \text{if } x_i < -a \end{cases}$$

$$y_i = 1 + \frac{1}{4}(x_i + 1)$$

$$f_4(x^*) = f_4(1, 1, ..., 1) = 0.0$$

Penalized Function2:

$$f_5(x) = 0.1\{\sin^2(3\pi x_1) + \sum_{i=1}^{n-1}(x_i - 1)^2[1 + \sin^2(3\pi x_{i+1})] + (x_n - 1)^2[1 + \sin^2(2\pi x_n)]\} + \sum_{i=1}^{n} u(x_i, 5, 100, 4)$$

where $|x_j| \leq 50.0$, and

$$f_5(x^*) = f_5(1, 1, ..., 1) = 0.0$$

The coefficients of SPSO, MPSO-TVAC, CLPSO, ICPSO and PID-PSO are set as follows:

The inertia weight w is decreased linearly from 0.9 to 0.4 in SPSO and MPSO-TVAC, while for PID-PSO, inertia weight is chosen with Eq.(80) and

Eq.(81). Two accelerator coefficients c_1 and c_2 are both set to 2.0 with SPSO, as well as in MPSO-TVAC, ICPSO and PID-PSO, c_1 decreased from 2.5 to 0.5,while c_2 increased from 0.5 to 2.5. Total individuals are 100, and v_{max} and a_{max} are both set to the upper bound of domain. The dimension is set to 30 and 100. Each experiment the simulation run 30 times while each time the largest evolutionary generation is 1500 and 5000 respectively. If other parameters not mentioned before, please refer to the corresponding references[17][13][14].

Tab.1 and Tab.2 are the comparison results of the benchmark functions under the same evolution generations respectively. Fig.3 to Fig.12 provide a details of the comparison results among the five methods.

From Tab.1, PID-PSO is superior to other algorithms in Rosenbrock and Rastrigin, while for Ackley and Penalized Function1, it's performance is only worse than ICPSO, but equivalent to MPSO-TVAC, and superior to SPSO and CLSPO. For Penalized Function2, PID-PSO is the worst algorithm. This phenomenon shows that PID-PSO is not suit for problems with small dimension.

For Tab.2, the performance of PID-PSO is very exciting, and is superior to other four algorithms only except for Ackley. Ackley has an exponential term that covers its surface with numerous local minima. The complexity of this function is moderated. An algorithm that only uses the gradient steepest descent will be trapped in a local optima, but any search strategy that analyzes a wider region will be able to cross the valley among the optima and achieve better results. However, Ackley tends to be an unimodal function with a large dimension because $\lim_{n\to\infty} exp(\frac{1}{n}\sum_{k=1}^{n}\cos 2\pi x_k) = 0$. This special issue also demonstrates that PID-PSO is not suit for the unimodal optimization problems.

Based on the above analysis, we can draw the following conclusion: PID-PSO is suit for high-dimensional multi-modal functions with many local optima.

5 CONCLUSION

PID-PSO is a new PSO variation by incoporating PID controllers to improve the population diversity. with support set theory, it provides more probability to escaping from a local optimum. Furthermore, parameter selection strategies are also discussed with stability analysis. Simulation results show the proposed PID-PSO is fit for high-dimensional multi-modal functions significantly. Further research topic includes the discrete PID-PSO and applications.

TABLE 1
Comparison Results for Benchmark Function on Dimension 30

Function	*Algorithm*	Mean Value	Standard Deviation
Rosenbrock	SPSO	5.6170e+001	4.3584e+001
	MPSO-TVAC	3.3589e+001	4.1940e+001
	CLPSO	5.1948e+001	2.7775e+001
	ICPSO	2.2755e+001	1.9512e+001
	PID-PSO	1.9757e+001	2.3479e+000
Rastrigin	SPSO	1.7961e+001	4.2276e+000
	MPSO-TVAC	1.5471e+001	4.2023e+000
	CLPSO	2.6818e+001	7.3875e+000
	ICPSO	1.2138e+001	2.1390e+000
	PID-PSO	4.3807e+000	2.8982e+000
Ackley	SPSO	5.8161e-006	4.6415e-006
	MPSO-TVAC	7.5381e-007	3.3711e-006
	CLPSO	5.6159e-006	4.9649e-006
	ICPSO	9.4146e-015	2.9959e-015
	PID-PSO	9.9638e-007	2.7760e-006
Penalized Function1	SPSO	6.7461e-002	2.3159e-001
	MPSO-TVAC	1.8891e-017	6.9756e-017
	CLPSO	1.0418e-002	3.1898e-002
	ICPSO	1.7294e-032	2.5762e-033
	PID-PSO	6.3309e-016	9.6331e-016
Penalized Function2	SPSO	5.4943e-004	2.4568e-003
	MPSO-TVAC	9.3610e-027	4.1753e-026
	CLPSO	1.1098e-007	2.6748e-007
	ICPSO	1.7811e-032	1.1537e-032
	PID-PSO	2.1974e-003	4.6326e-003

TABLE 2
Comparison Results for Benchmark Function on Dimension 100

Function	*Algorithm*	Mean Value	Standard Deviation
Rosenbrock	SPSO	4.1064e+002	1.0584e+002
	MPSO-TVAC	2.8517e+002	9.8129e+001
	CLPSO	3.7129e+002	9.0863e+001
	ICPSO	1.5630e+002	3.4292e+001
	PID-PSO	1.2287e+002	3.6026e+001
Rastrigin	SPSO	9.3679e+001	9.9635e+000
	MPSO-TVAC	8.4478e+001	9.4568e+000
	CLPSO	2.3827e+002	3.1276e+001
	ICPSO	7.8701e+001	7.3780e+000
	PID-PSO	1.0400e+001	4.1613e+000
Ackley	SPSO	3.3139e-001	5.0105e-001
	MPSO-TVAC	4.6924e-001	1.9178e-001
	CLPSO	5.7193e-001	5.7978e-001
	ICPSO	2.3308e+000	2.9163e-001
	PID-PSO	4.6621e-001	5.3628e-001
Penalized Function1	SPSO	2.4899e+000	1.2686e+000
	MPSO-TVAC	2.3591e-001	1.9998e-001
	CLPSO	4.6653e+000	1.4842e+000
	ICPSO	8.4038e-002	1.0171e-001
	PID-PSO	6.7518e-007	7.9907e-007
Penalized Function2	SPSO	3.8087e+001	1.8223e+001
	MPSO-TVAC	3.7776e-001	6.1358e-001
	CLPSO	4.7576e+001	2.6205e+001
	ICPSO	7.3122e-001	1.0264e+000
	PID-PSO	3.3486e-002	8.5851e-002

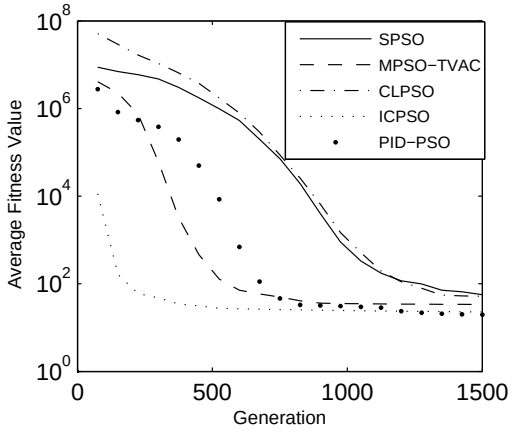

FIGURE 3
Comparison results of Rosenbrock on dimension 30.

ACKNOWLEDGMENTS

The authors would like to thank the Doctoral Scientific Research Starting Foundation of Taiyuan University of Science and Technology under No.20082010, and the National Natural Science Foundation of China under Grant No. 60674104.

REFERENCES

[1] R. Eberhart and J. Kennedy, A new optimizer using particle swarm theory, Proceedings of 6^{th} International Symposium on Micro Machine and Human Science, (1995) 39-43.

[2] J. Kennedy and R. Eberhart, Particle swarm optimization, Proceedings of ICNN'95 - IEEE International Conference on Neural Networks, (1995) 1942–1948.

[3] K.E. Parsopoulos and M.N. Vrahatis, Particle swarm optimization method for constrained optimization problems. In: P. Sincak, J. Vascak, V. Kvasnicka and J. Pospichal editored: Intelligent Technologies - Theory and Applications - New Trends in Intelligent Technologies, (2002) 214-220.

[4] Q.M. Liu, and W. Lv, The forecasting residual life of underground pipeline based on particle swarm optimisation algorithm, International Journal of Bio-Inspired Computation, 1 (4) (2009) 270C275.

[5] B. Liu, L. Wang and Y.H. Jin, An effective hybrid particle swarm optimization for no-wait flow shop scheduling, International Journal of Advanced Manufacturing Technology, 31 (9-10) (2007) 1001-1011.

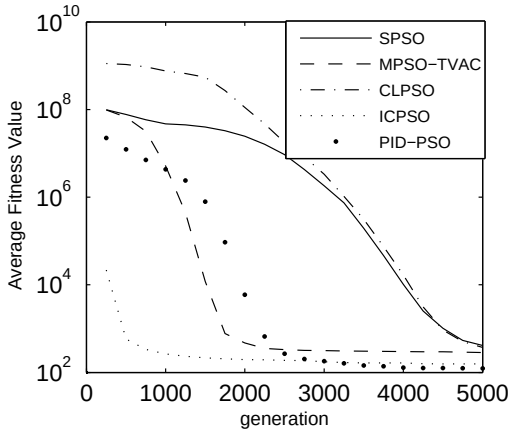

FIGURE 4
Comparison results of Rosenbrock on dimension 100.

[6] P.Y. Yin, A discrete particle swarm algorithm for optimal polygonal approximation of digital curves, Journal of Visual Communication and Image Representation, 15 (2) (2004) 241-260.

[7] J. Riget and J.S. Vesterstrϕ, A diversity-guided particle swarm optimizer - the ARPSO, EVALife Technical Report No.2002-02, (2002).

[8] R. He, Y. WANG, Q. WANG, et al., An improved particle swarm optimization based on self-adaptive escape velocity, Journal of Software, 16 (12) (2005) 2036-2044.

[9] Z. Cui, X. Cai, J. Zeng and G. Sun, Particle swarm optimization with FUSS and RWS for high dimensional functions, Applied Mathematics and Computation, 205 (1) (2008) 98-108.

[10] R. Mendes, J. Kennedy and J.Neves,The fully informed particle swarm: simpler, maybe better, IEEE Transactions on Evolutionary Computation, 8 (3) (2004) 204-210.

[11] J. Kennedy, Small worlds and mega-minds: effects of neighborhood topology on particle swarm performance, Poceedings of the 1999 Congress on Evolutionary Computation, (1999) 1931-1938.

[12] M. Lϕvbjerg, T.K. Rasmussen and T. Krink, Hybrid particle swarm optimiser with breeding and subpopulations, Proceedings of the third Genetic and Evolutionary Computation Conference, (2001).

[13] J. Zeng, Z. Cui, Particle swarm optimizer with integral controller, Proceedings of 2005 International Conference on Neural Networks and Brain, (2005) 1840-1842.

[14] Z. Cui, J. Zeng, G. Sun, Adaptive integral-controller particle swarm optimization using accelerator feedbackJournal of Chinese Computer Systems28 (5) (2007) 855-860(in Chinese)

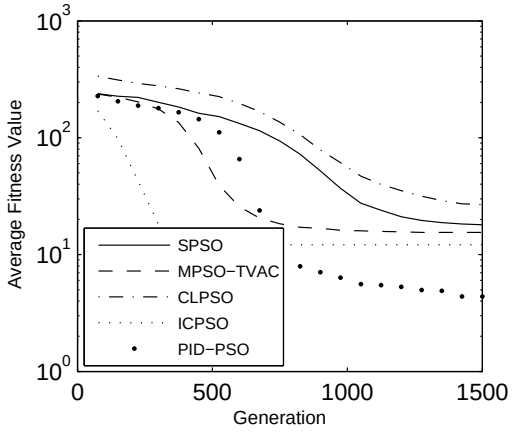

FIGURE 5
Comparison results of Rastrigin on dimension 30.

[15] F.Bergh, An analysis of particle swarm optimizers, South Africa: University of Pretoria, (2001).

[16] A. Ratnaweera, S. Halgamuge and H. Watson, Self-organizing hierarchical particle swarm opitmizer with time-varying acceleration coefficients, IEEE Transactions on Evolutionary Computation, 8 (3) (2004) 240-255.

[17] J. Liang, A. Qin, P. Suganthan, et al., Comprehensive learning particle swarm optimizer for global optimization of multimodal functions, IEEE Transactions on Evolutionary Computation, 10 (3) (2006) 281-295.

[18] X. Yao, Y. Liu and G.M. Lin, Evolutionary programming made faster', IEEE Transactions on Evolutionary Computation, 3 (2) (1999) 82-102.

[19] Y.W. Shang and Y.H. Qiu, A note on the extended Rosenbrock function, Evolutionary Computation, 14 (1) (2006) 119-126.

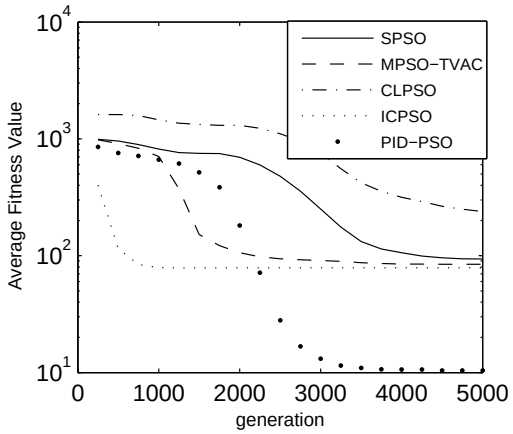

FIGURE 6
Comparison results of Rastrigin on dimension 100.

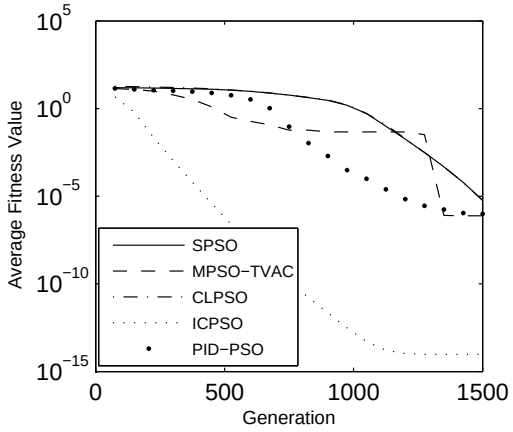

FIGURE 7
Comparison results of Ackley on dimension 30.

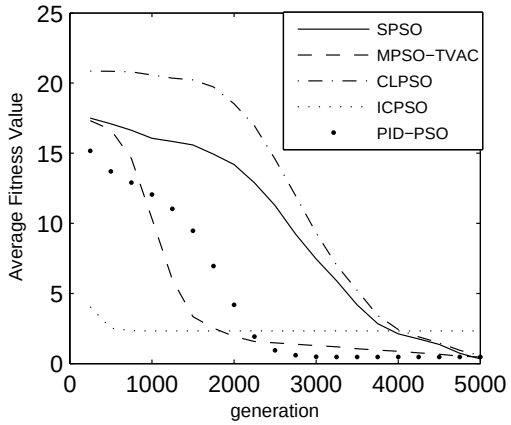

FIGURE 8
Comparison results of Ackley on dimension 100

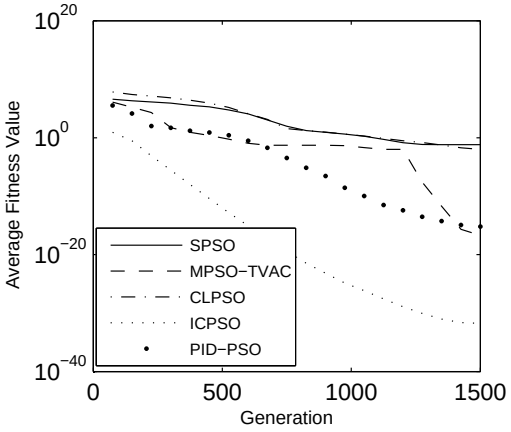

FIGURE 9
Comparison results of Penalized Function1 on dimension 30

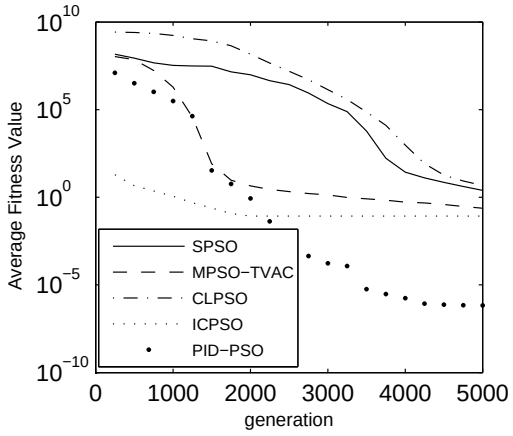

FIGURE 10
Comparison results of Penalized Function1 on dimension 100

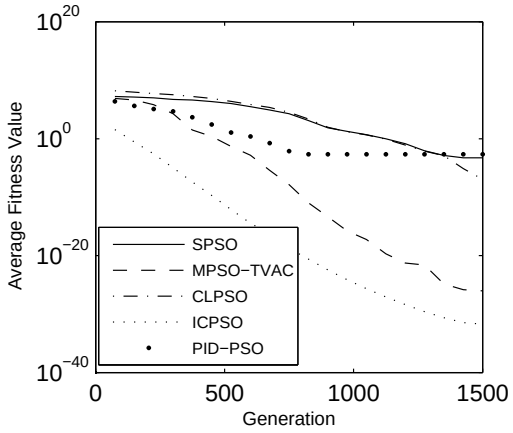

FIGURE 11
Comparison results of Penalized Function2 on dimension 30

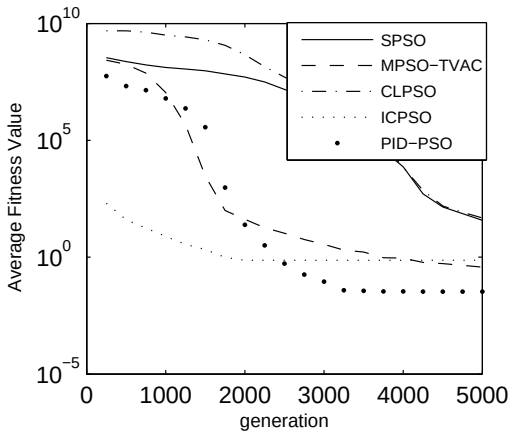

FIGURE 12
Comparison results of Penalized Function2 on dimension 100